Available online at www.sciencedirect.com

SciVerse ScienceDirect

Energy Procedia 37 (2013) 1267 – 1274

Energy Procedia

GHGT-11

Dynamic measurements of CO_2 flow in water saturated porous medium at low temperature using MRI

Mingjun Yang, Yongchen Song*, Ningjun Zhu, Yuechao Zhao, Yu Liu, Lanlan Jiang

Key Laboratory of Ocean Energy Utilization and Energy Conservation of Ministry of Education, Dalian University of Technology, No.2 Linggong Road, Ganjingzi District, Dalian 116024, China

Abstract

The present study provides some important thermodynamic and kinetic data for the CO_2 hydrate formation in flow system. Images were obtained dynamically using Magnetic resonance imaging (MRI) system, with a fast spin-echo multi-slice scan sequence (FSEMS). The CO_2 hydrate dissociation rate was quantified using MRI mean intensity of liquid water. The saturation of residual liquid water, CO_2 hydrate and CO_2 gas during the dissociation of CO_2 hydrate were also quantified using MRI data. The highest CO_2 hydrate saturation was 58% in the first process, and 26% for the second process in this investigation.

Keywords: CO_2 hydrate; flow; porous medium; MRI

1. Introduction

International Energy Agency (IEA) proposed that if the target of climate change control was obtained without CCS, the total cost will increase 70% than with CCS in 2050[1].Hydrate-based CO_2 separation as a promising option for fossil fuel power plant is attracting people concentration, which is a novel concept that aims to use CO_2 hydrate to trap CO_2 molecules in a lattice of water molecules. This process is carried out by forming the hydrate form CO_2/N_2 or CO_2/H_2 gas mixture under high pressure and low temperature. After the CO_2 hydrate is formed, solid hydrate was separated and dissociated to releasing CO_2[2].Department of Energy of USA considers it is the most promising long-term CO_2 capture technology identified to date because its energy penalty may be as small as 6% to 8% is currently in the

* Corresponding author. Tel.: +86-411-84709093; fax: +86-411-84708015.
E-mail address: songyc@dlut.edu.cn.

doi:10.1016/j.egypro.2013.06.001

R&D phase[3]. Wong *et al.* believed that potential cost reduction of CO_2 production for hydrate based option is 45% compare to the current chemical absorption technology in 15a later[4].

Since the hydrate based option was proposed to separate CO_2[5,6], lots of investigations were carried out to mitigate hydrate formation conditions and increase hydrate formation rate. Gas hydrates from CO_2/N_2 and CO_2/H_2 gas mixtures were formed in a semi-batch stirred vessel at constant pressure and temperature of 273.7 K by Linga *et al.* [7].The rate of hydrate growth from CO_2/H_2 mixtures was found to be the fastest. In both mixtures gas CO_2 was found to be preferentially incorporated into the hydrate phase. In 2010 they reported that the gas uptake and CO_2 recovery for flue gas mixture in the presence of THF obtained in this work was higher than that reported in the literature with tetra-n-butyl ammonium bromide and tetra-n-butyl ammonium fluoride[8]. One of the key elements for successful development of hydrate technology is the improvement of gas/liquid contact[9]. Although hydrate crystallization is able to capture CO_2, the power required for mechanical agitation was found to be very significant. If the hydrate process is to be used industrially then hydrate crystallization must be carried out without mechanical agitation[8]. Micro-scale investigation showed that porous medium can provide favorable carrier for hydrate formation. Seo *et al.,* found that dispersed water in the silica gel pore system reacts readily with the gas, thus obviating the need for a stirred reactor and excess water[10]. Adeyemo concluded that a near four-fold increase in moles of gas incorporated in the hydrate per mole of water, and the improved water-to-hydrate conversion is obtained with pore-dispersed water. He also found that CO_2 recovery improved from 42% for stirred-tank studies to 51% for the optimum silica determined in his study, and THF optimum concentration using in silica is different from that in stirred-tank experiments [11]. Kang *et al.* found that obtained gas from the dissociation of hydrate contains more than 95 mol% of CO_2 (70 mol% in bulk water hydrate), which further validated the feasibility of CO_2 separation process by hydrate formation in porous silica gel[12].

MRI is an effective tool for investigations in physical, chemical, life, and clinical sciences. In order to obtain high precious data and make visible measurement, MRI has been used for studying the hydrate. Having designed and constructed a high-pressure vessel to safely withstand 40MPa, Hirai *et al.* observed CO_2 hydrate growth in a water droplet injected into liquid CO_2 at 20MPa with the vessel. Their experiments demonstrated not only the effective performance of the apparatus but also the perfect performance of MRI for hydrate investigations[13]. Then they measured hydrate thickness growth with MRI and the phenomenon applied to advanced CO_2 ocean dissolution technology[14]. The presence of porous media may be a challenge for the hydrate investigation using MRI, the baffle was quickly disappeared with the following works[15-16]. Kvamme *et al.* applied MRI to visualize the conversion of CH_4 hydrate within Bentheim sandstone matrix into the CO_2 hydrate[17]. And then they carried some experiments to investigate the rates and mechanisms of hydrate formation in coarse-grain porous media[18]. Many of these experiments were conducted in a sample holder fitted within a MRI instrument that allowed for a unique method of monitoring hydrate formation by the loss of signal intensity as water and free gas are converted into a solid phase. Most of the following experiments done by them were also focused on the exchange of carbon dioxide for methane in the hydrate[19,20,21,22].

Although lots of studies have been carried to investigate CO_2 separate based hydrate formation process, they are mostly focused on thermodynamic properties. There is only very limited information on the kinetic data of CO_2 hydrate formation, especially for the conditions that CO_2 flowing in porous medium. With the background of CCS, this study focus on analyzing the hydrate formation process when CO_2 flow in porous medium at different pressure, temperature, which may be helpful to understanding CO_2 capture technology based on hydrate formation. The present study will provides some important thermodynamic and kinetic data for the CO_2 hydrate formation in flow system. It also can be used to provide fundamental data for the conceptual design of the hydrate-based CO_2 capture process. The knowledge obtained from this work is sufficiently general and is expected to be useful in the other applications.

2. Experimental investigation

2.1. Experimental apparatus

The experimental apparatus consisted of five subsystems: (A) the high-pressure vessel; (B) the MRI system to visualize CO_2 hydrate formation and dissociation; (C) the data acquisition system to measure pressure and temperature; (D) water, and carbon dioxide high-pressure pumps to provide pore pressure; (E) a low-temperature cooling system to keep the vessel at low temperature (Fig 1).

An important criterion of the high-pressure vessel is that it must be made of non-magnetic material and have a relatively large inside volume. The vessel is made of Polyimide and its design pressure is 12MPa. The effective size is Φ15×200 mm; the total size is Φ38×314 mm. The vessel is surrounded by a jacket which can heat or cool the vessel. The MRI operated at a resonance of 400MHz, 9.4T, to measure hydrogen. ^{1}H MRI produces images of hydrogen contained in liquids, but does not image hydrogen contained in solids such as crystals or ice because of their much shorter relaxation times. The rock is not imaged because it is solid and contains little, if any, hydrogen. This makes MRI a potent tool to distinguish between solid hydrate and the liquid mixture from which the hydrate forms.

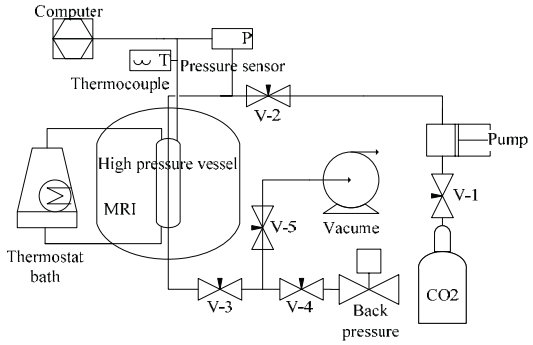

Fig. 1. Schematic diagram of the experimental apparatus

The pressure transducers produced by Nagano, Japan Co., Ltd are connected to the vessel. The estimated errors of pressure are ±0.1MPa, respectively. Temperature and pressure signals from thermocouples and pressure sensors are collected by A/D module (Advantech CO., Ltd.) and sent to the PC, then; the data are processed by Monitor and Control Generated System. The high precision Syringe pump (260D), produced by Teledyne Isco Inc., America, is used to increase pore pressure and keep CO2 flowing constantly. Back pressure regulator (BP-2080-M) is made by JASCO Corporation, Japan. In order to acquire a stable-temperature, a large-scale and high-precision thermostat bath (produced by JULABO Labortechnik GmbH) filled with FC-40 (supplied by 3M Company) was introduced to control temperature precisely, in which temperature is regulated and controlled by a heater and a refrigerator. The temperature stability of the bath (F-25 me) was ±0.01K.

2.2. Experimental procedures

The glass beads used in this study was produced by As-One Co., Ltd., Japan. CO_2 (99.9%) was provided singly by Dalian Guangming special gas co., Ltd. The de-ionized water was used in all

experiments. After packed the glass beads into the vessel tightly with de-ionized water, the vessel was reconnected to the system and the de-ionized water was partly displaced with CO_2 gas. A vacuum pump was used to discharge the gas in the vessel, then the bath temperature was decreased to designed value and the MRI began to obtain images. CO_2 was then injected slowly into the vessel and kept back pressure at designed value. Once the pressure was stably, the pump was used to drive CO_2 flow in the vessel at designed value. The flow process was ended when there was neither pressure change nor image change in the vessel. The temperature was then increased gradually to make hydrate decompose. When the images turned to the same as the initial ones, the pump was powered on again to repeat the experiment. All the images were acquired with fast spin-echo multi-slice scan (FSEMS) sequences, which can give high-quality, artifact-free images of high resolution and signal-to-noise ratio. Scanning parameters were adjusted to produce proton density-weighted images. Echo time (TE) was 5.62 ms, and repetition time (TR) was 2000 ms. Total acquisition time of each scan was 36 s. Field of view (FOV) was selected at the vertical center section of the imaging vessel, and the size was 40×40 mm. The image data matrix was 128×128, and spatial resolution was 0.31×0.31×1mm.

3. Results and discussion

In order to investigate the hydrate formation character when CO_2 flowing in porous medium at low temperature, MRI was used to image the sample in the vessel. Glass bead (BZ-01, 0.105-0.125mm) was used to simulate the porous medium, which porosity is 36.4%. The sagittal plane was selected to display the experimental process in this paper. The initial experimental pressure (p) and temperature (T) were 275.25 K and 4.0 MPa, and the flow rate was 1 ml/min.

Fig 2 shows the water distribution in the vessel during CO_2 hydrate formation and dissociation when CO_2 flowing in porous medium. The bright signal in images reflects the liquid water in the vessel. When liquid water turns to solid phase (hydrate), the bright signal will change to dark. About 19 minutes later, CO_2 reach to FOV of MRI. The water distribution (bright signal) in the vessel changed due to the CO_2 drive water and the formation of CO_2 hydrate. The water signal disappeared in two minutes, which implied the end of CO_2 hydrate formation in this experiment. The residual bright signal near the vessel wall indicated the water was not totally consumed.

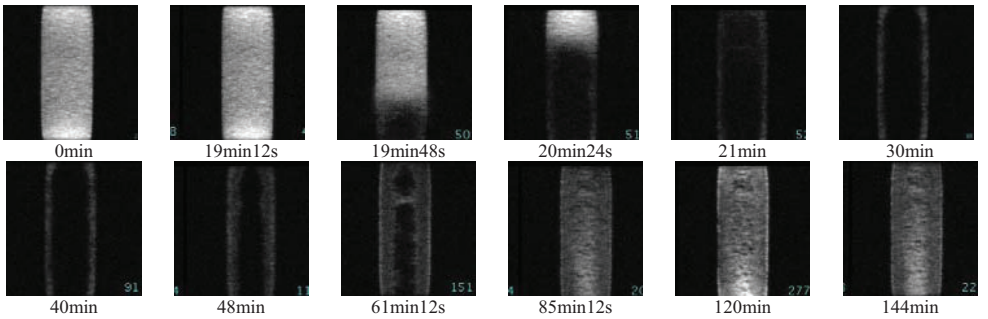

Fig. 2. Distribution of water saturation in the porous media caused by CO_2 flowing and hydrate formation (first cycle)

The phenomena mainly caused by the formation of CO_2 hydrate which blocked the pores and prevented the contact of water and CO_2. The pressure and mean intensity of water in vessel changed with time was shown in Figure 3, which also showed the water was not totally consumed by the mean intensity. Since there was no signal change in vessel 21 minutes later and hydrate will not formed as kept injecting CO_2,

the CO_2 flowing was stopped 30mintues later. And the heating procedure started in 10 minutes at 1K/min, which can make CO_2 hydrate decomposition. The temperature was increased to 284K to make hydrate dissociate. Fig 2 shows the dissociation process of CO_2 hydrate began when the temperature was increased to 281K (8minurtes later). The CO_2 hydrate dissociated firstly in the around the wall of vessel in the experiment. The CO_2 hydrate was completely dissociate in 75 minutes later. The quantitative data for the experiment was shown in Figure 3, and discusssed detailed following.

Figure 3 shows the vessel pressure changes which imply the consumption and release of CO_2 during hydrate formation and dissociation, and the comparison of the MRI mean intensity of liquid water and the pressure in the vessel was also shown in it. The decrease of vessel pressure after the injection stopped was due to the hydrate formation in the vessel that was not included in the FOV. If the injection time was extended, the pressure decrease disappeared. Since the condition did not affect the experimental result, the long-time injection experiment was not carried in this study. While the pore water was consumed when hydrate formation and caused the decrease of MRI mean intensity. About 26 minutes later, hydrate formation was finished. The MRI mean intensity of water in the vessel was fairly constant throughout the experiment from 28 minutes to 42minutes. Then the vessel was heated, and due to the high heating rate the increase of MRI mean intensity indicated CO_2 hydrate began dissociated 42 minutes later. The water saturation and pressure increased simultaneously during the heating process, this can determined the CO_2 hydrate formed as CO_2 flowing in water saturated porous medium with low temperature. The hydrate dissociation process finished in FOV 80 minutes later, and then the mean intensity value kept constant.

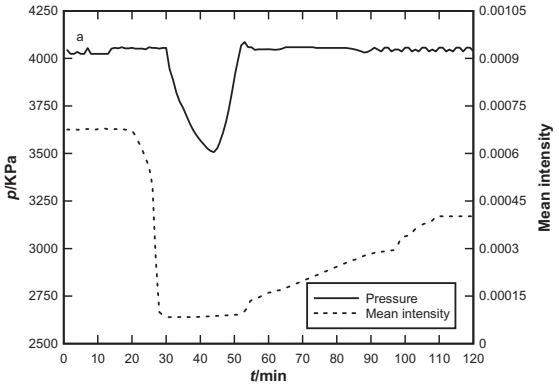

Fig. 3. MRI mean intensity of water and vessel pressure change during the formation and dissociation of CO_2 hydrate

The CO_2 hydrate dissociation rate was also quantified using MRI mean intensity of liquid water. The saturation of residual liquid water and CO_2 hydrate during the dissociation of CO_2 hydrate were showed in Fig 4. In this study, the initial water saturation was 100%, and the value used to calculate hydrate saturation was the water saturation after the hydrate dissociated (about 59%). Saturation of residual liquid water can be calculated using MRI mean intensity. Since the water saturation changed during formation process due to the CO_2 injection, the hydrate saturation cannot be calculated in hydrate formation process. The expression of residual water saturation was as follow:

$$S_W = \frac{I_i \times S_{W0}}{I_0} \times 100\% \quad (1)$$

Where S_{W0} is the initial water saturation, I_0 and I_i were the MRI mean intensity of liquid water at initial time and i minutes.

Since the hydrates concentrate former gas [at standard temperature and pressure (STP)] by as much as a factor of 164 and 0.8 water, we assumed that one volume of water can convert into 1.25 volume hydrate (Sloan, 1998). The saturation of CO_2 hydrate and CO_2 gas can be calculated using the follow equations:

$$S_h = 1.25 \times \frac{(I_0 - I_i) \times S_{W0}}{I_0} \times 100\% \quad (2)$$

$$S_{CO2} = 1 - S_W - S_h \quad (3)$$

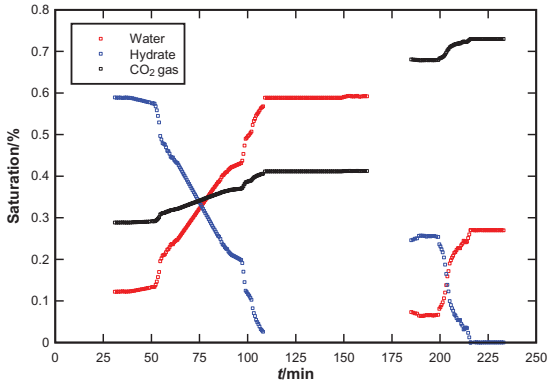

Fig. 4. Saturation of residual water, hydrate and CO_2 gas during hydrate dissociation process

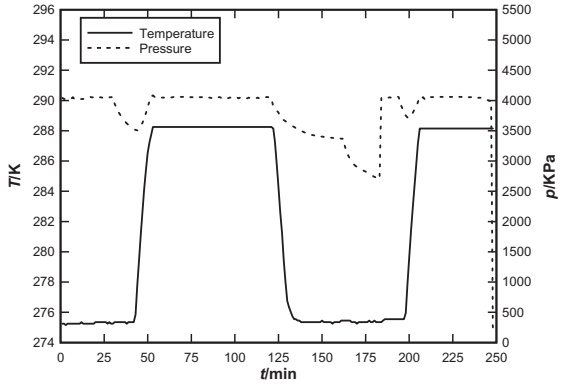

Fig. 5. Pressure and temperature changes in the experiment

The saturations were calculated for two hydrate dissociation processes using above equations, and the results were shown in Figure 4. The highest CO_2 hydrate saturation was about 59% in this study presenting in the first process, and 26% for the second process. When the hydrate dissociation process

finished, the hydrate saturation get to 0. And the water saturation shows the highest value, which reflects the residual water saturation after the first and second CO_2 injection (59% and 27%). Fig 4 also showed the saturation of CO_2 gas.

Since the back pressure was kept at 4 MPa, CO_2 released from hydrate was partly effluent from the vessel. The hydrate formation was not significant as temperature decreased again (165min). When the CO_2 flowing in the vessel again at 180 min, the water was flushd again due to the high pressure difference. And CO_2 hydrate formed again. The vessel was heated again at 198min, and the hydate decomposition finished at 219 min, as shown in Fig 5.

4. Conclusions

Since MRI is an effective tool for hydrate investigations, experiments were carried out to study CO_2 hydrate formation and dissociation as CO_2 flowing in water saturated porous medium at low temperature. A new vessel was designed to satisfy the demands of high pressure and no influence on the magnetic signal used in the experiments. The vessel pressure was recorded during hydrate formation and dissociation, which was used to compare to MRI mean intensity of liquid water. The results indicated that the MRI could visualize water movement caused by water displacement and hydrate formation. The hydrate dissociation process can be detected and quantitative analyzed by MRI. The saturation of residual water, CO_2 hydrate and CO_2 gas during the dissociation of CO_2 hydrate were calculated using MRI mean intensity of liquid water, which can indicated hydrate dissociation rate quantitatively. Since the water saturation changed during formation process due to the CO_2 injection, the hydrate saturation cannot be calculated in hydrate formation process. The CO_2 hydrate dissociation rate was quantified using MRI mean intensity of liquid water. The water saturation after the two hydrate dissociated process was about 59% and 27%. The highest CO_2 hydrate saturation was 59% in this study presenting in the first process, and 26% for the second process. The gas saturation shows the highest value for the first and second CO_2 injection process (41% and 73%). The pressure difference between inlet and outlet of the vessel indicated that hydrate can blocked the pores medium. And since the limitation of experimental system, the accurate location of block cannot be detected in this study.

Acknowledgements

This project is financially supported by Key program of National Natural Science Foundation of China (50736001), the National Natural Science Foundation of China (51106018), the National High Technology Research and Development Program of China (2009AA063402), the Scientific Research Foundation for Doctors of Liaoning Province (20111026) and the Fundamental Research Funds for the Central Universities of China.

References

[1] IEA. *Energy Technology Perspectives*. Paris: France; 2008.

[2] Yang HQ, Xu ZH, Fan MH, Gupta R, Slimane RB, Bland AE, Wright I. Progress in carbon dioxide separation and capture: A review. *J Environ Sci* 2008; **20**:14–27.

[3] Elwell L C, Grant W S. Technology options for capturing CO_2-Special Reports, *Power* 2006, **150**.

[4] Wong S, Bioletti R. *Carbon Dioxide Separation Technologies*, Carbon & Energy Management Alberta Research Council Edmonton, Alberta, T6N 1E4, Canada, 2002.

[5] Spencer D. Integration of an advanced CO_2 separation process with methods for disposing of CO_2 in oceans and terrestrial deep aquifers. *Proceedings of the 26 International Conferences on Greenhouse Gas Control Technologies*, 1998.
[6] Spencer D, Tam S. An engineering and economic evaluation of a CO_2 hydrate separation system for shifted synthesis gas. *Proceedings of 16th Annual International Pittsburgh Coal Conference*, 1999.
[7] Linga P, Kumar R, Englezos P. Gas hydrate formation from hydrogen/carbon dioxide and nitrogen/carbon dioxide gas mixtures. *Chemical Engineering Science* 2007; **62**: 4268-4276
[8] Linga P, Kumar R, Lee J, Ripmeester J, Englezos P. A new apparatus to enhance the rate of gas hydrate formation: Application to capture of carbon dioxide. *International Journal of Greenhouse Gas Control* 2010; **4**: 630–637.
[9] Mori, Y. H.,. Recent Advances in Hydrate-based Technologies for Natural gas Storage-A Review. *Journal of Chemical Industry and Engineering* 2003; **54**, 1-17.
[10] Seo Y. Efficient Recovery of CO_2 from Flue Gas by Clathrate Hydrate Formation in Porous Silica Gels. *Environ Sci Technol* 2005; **39**: 2315-2319.
[11] Adeyemo A. Post Combustion Capture of Carbon Dioxide through Hydrate Formation in Silica Gel Column. University of British Columbia, Vancouver. 2008.
[12] Seong-Pil Kang, Yutaek Seo, Wonho Jang, Yongwon Seo. *Gas Hydrate Process for Recovery of CO_2 from Fuel Gas*. The ninth International Conference on Chemical & Process Engineering. Rome, Italy. 2009.
[13] Hirai S, Kuwano K, Ogawa K, Iriguchi N, Okazaki K. High-pressure magnetic resonance imaging up to 40 MPa. *Magnetic Resonance Imaging* 2000; **18**: 221–225.
[14] Hirai S, Tabe Y, Kuwano K, Ogawa K, Okazaki K. MRI measurement of hydrate growth and an application to advanced CO_2 sequestration technology, *Annals of the New York Academy of Sciences* 2000; **912**: 246 – 253.
[15] Baldwin BA, Moradi-Araghi A, Stevens JC. Monitoring hydrate formation and dissociation in sandstone and bulk with magnetic resonance imaging, *Magnetic Resonance Imaging* 2003; **21**: 1061–1069.
[16] Yang MJ, Song YC, Zhao YC. MRI measurements of CO_2 hydrate dissociation rate in a porous medium. *Magnetic Resonance Imaging*. 2011; **29**: 1007-1013.
[17] Kvamme B, Graue A, Buanes T, Kuznetsova T, Ersland G. Storage of CO_2 in natural gas hydrate reservoirs and the effect of hydrate as an extra sealing in cold aquifers. *International journal of greenhouse gas control* 2007; **1**: 236–246.
[18] Stevens JC, Howard JJ, Baldwin BA, Ersland G, Husebø J, Graue A. Experimental hydrate formation and gas production scenarios based on CO_2 sequestration, *Proceedings of the 6th International Conference on Gas Hydrates*, Vancouver, British Columbia, Canada 2008.
[19] Husebø J, Ersland G, Graue A, Kvamme B. Effects of salinity on hydrate stability and implications for storage of CO_2 in natural gas hydrate reservoirs, *Energy Procedia* 2009; **1**: 3731–3738.
[20] Ersland G, Husebo J, Graue A, Kvamme B. Transport and storage of CO_2 in natural gas hydrate reservoirs. *Energy Procedia* 2009; **1**: 3477–3484.
[21] Ersland G, Husebo J, Graue A, Baldwin BA, Howard J, Stevens J. Measuring gas hydrate formation and exchange with CO2 in Bentheim sandstone using MRI tomography. *Chemical Engineering Journal* 2009; **158**: 25–31.
[22] Baldwin BA, Stevens J, Howard JJ, Graue A, Kvamme B, Aspenes E, Ersland G, Husebø J, Zornes DR. Using magnetic resonance imaging to monitor CH_4 hydrate formation and spontaneous conversion of CH_4 hydrate to CO_2 hydrate in porous media. *Magnetic Resonance Imaging* 2009; **27**:720-726.